ISSN 0020-4412, Instruments and Experimental Techniques, 2021, Vol. 64, No. 2, pp. 277–284. © Pleiades Publishing, Ltd., 2021.
Russian Text © The Author(s), 2021, published in Pribory i Tekhnika Eksperimenta, 2021, No. 2, pp. 107–114.

GENERAL EXPERIMENTAL TECHNIQUES

Inspection Probes of a Ferromagnetic Resonance Scanning Spectrometer

B. A. Belyaev[a,b,*], N. M. Boev[a,b], A. A. Gorchakovsky[a,b], and R. G. Galeev[c,d]

[a] *Kirensky Institute of Physics, Siberian Branch, Russian Academy of Sciences, Krasnoyarsk, 660036 Russia*

[b] *Siberian Federal University, Krasnoyarsk, 660074 Russia*

[c] *Reshetnev Siberian State University of Science and Technology, Krasnoyarsk, 660037 Russia*

[d] *AO NPP Radiosvyaz, Krasnoyarsk, 660021 Russia*

*****e-mail: belyaev@iph.krasn.ru*

Received August 11, 2020; revised August 17, 2020; accepted August 25, 2020

Abstract—The design of inspection probes for a scanning ferromagnetic resonance spectrometer, which are designed for recording the absorption spectra of electromagnetic energy by local areas of thin magnetic films, is described. The degree of locality is determined by the diameter of the measuring hole of the probe in the range of 0.1–1.0 mm. The sensitivity of the device is significantly increased due to the miniaturization of the heterogeneous measuring resonator and its comparatively high Q factor. A set of replaceable probes makes it possible to cover the frequency range of 0.1–6.0 GHz, the signal-to-noise ratio for a probe with a hole diameter of 0.8 mm, which was measured on a permalloy film with a thickness of 5 nm, is at least 20 dB.

DOI: 10.1134/S0020441221010218

INTRODUCTION

Thin magnetic films (TMFs) are widely used in devices for recording and reading information [1, 2]; they are used for constructing sensors of weak magnetic fields [3, 4], creating frequency-selective devices [5, 6] and various spintronics-based devices [7], as well as nonlinear microwave devices, such as frequency multipliers [8]. The characteristics of such devices depend not only on the magnetic parameters of TMFs, but also on the degree of inhomogeneity of these parameters over the area of films, which is determined by the quality of substrates and the specific sample-manufacturing technology.

It is obvious that the development of any technology for depositing magnetic films is impossible without equipment that allows measurements of their characteristics on local areas of the obtained samples and, primarily, the parameters of the magnetic anisotropy and attenuation of the magnetization precession. In this case, one of the most efficient and accurate methods is the ferromagnetic resonance (FMR) method [1, 9, 10].

Frait [11] proposed to study local areas of TMFs with the FMR method using a hole in the wall of a cavity resonator. A selected area of a thin magnetic film was applied to the hole on the outside of the resonator, and the hole served as a localized source of a high-frequency magnetic field. Using this idea, Sukhu developed a design of an apparatus for measuring the FMR spectra on local areas of films, which was called the "microwave magnetic microscope" [1, 12]. At the same time, only the replacement of the cavity resonator with a microstrip resonator has led to a significant increase in both the sensitivity of the measuring setup and the accuracy of recording spectra from local TMF areas [13]. This made it possible to develop an automated scanning FMR spectrometer, which can be used to observe the character of the inhomogeneity distributions of a number of magnetic characteristics over the sample area [13, 14].

Owing to the advent of a scanning FMR spectrometer, a number of new effects in magnetic films, which are not only of scientific but also practical importance, have been discovered and investigated. In particular, an excess of the magnetic susceptibility that is observed near the uniaxial magnetic-anisotropy field in a wide frequency range, which was called the nonresonant magnetic susceptibility, was found in [15]. The FMR in the quasi-equilibrium state of the magnetic moment of TMFs was detected and investigated [16]. A sharp change in the uniaxial magnetic-anisotropy magnitude and angle of direction near the edges of a TMF was revealed [17, 18], which is caused by the magnetic fields that exist at the ends of a magnetized sample [19]. It is shown that the vicinal and azimuthal interface angles of a single-crystal substrate, on which

a magnetic film is deposited, can be measured with a high accuracy [20]. Recently, a flexomagnetic effect was detected in a nonuniformly stressed magnetic film [21].

The sensitive element of the scanning FMR spectrometer is a microwave probe that consists of a metal case which houses a microstrip resonator on a substrate with a high permittivity. The resonator has a hole in the shield near the antinode of a high-frequency magnetic field and is the oscillatory circuit of a transistor microwave oscillator, which operates in the autodyne mode with an amplitude detector at the output [13, 14]. The change in a signal at the detector when scanning a DC magnetic field is proportional to the value of the microwave power absorption by the film area that is located under the measuring hole.

The sensitivity of probes with a microstrip resonator is higher compared to resonators. However, this sensitivity is not sufficient when measuring the parameters of films with a thickness less than 10 nm; therefore, signal accumulation is required, thus significantly increasing the measurement time. It is important to note that the size of the microstrip resonator increases in an inversely proportional manner to its resonant frequency, thus leading to a corresponding decrease in the sensitivity of the inspection probe.

In this paper, we present the designs of new miniature heterogeneous resonators and microwave probes based on them, whose sensitivity is increased by more than an order of magnitude; the sensitivity of all probes that operate in the frequency range of 0.1–6.0 GHz remains almost the same.

THE DESIGN OF THE MEASURING MICROWAVE PROBE

It is known [22] that the absorption of the electromagnetic energy by a sample placed in a microwave resonator is proportional to the imaginary part χ'' of its complex susceptibility. The minimum value of χ'' that can be detected by the spectrometer can be estimated by the formula:

$$\chi''_{\min} = \frac{KV}{\pi Q_0}\sqrt{\frac{kT_N\Delta f}{P}}. \quad (1)$$

Here, K is the coefficient of filling the resonator by the sample; V is the effective volume of the resonator, which is determined from the expression $W = Vh^2/(8\pi)$, where h is the amplitude of the high-frequency magnetic field on the sample and W is the total energy stored in the resonator; Q_0 is the unloaded resonator Q factor; k is the Boltzmann constant; T_N is the equivalent temperature of detector noises; Δf is the detector bandwidth; and P is the power of the microwave generator.

It follows from formula (1) that to increase the sensitivity of the spectrometer it is necessary to increase the Q_0/V ratio. However, given the fact that it is almost impossible to significantly increase the intrinsic Q factor of a miniature resonator, it is possible to increase the sensitivity of a scanning FMR spectrometer only by reducing the volume of the measuring resonator.

As already noted, the resonator is the oscillatory circuit of the microwave oscillator of the measuring probe, whose circuit diagram is shown in Fig. 1. The oscillator is a Colpitts oscillator based on a bipolar transistor Q_1, which is connected according to a common-base circuit. This allows minimization of the number of elements in the circuit and simplifies tracing the printed-circuit board of the probe. The optimal DC mode of the transistor is set by the trimming resistor R_1. A U-shaped oscillatory circuit with an inductance in the form of a small segment of a microstrip line is used in the circuit as a half-wave resonator. Series-connected capacitors C_2 and C_3, which form a high-frequency voltage divider, are connected to one end of the line, while a capacitor C_4 is connected to the other end. These capacitors, which are marked with asterisks on the diagram, adjust the frequency of the oscillator; by selecting the ratio of the capacitors C_2 and C_3, the optimal feedback in the oscillator is established to achieve the required sensitivity of the probe. It should be noted that at certain oscillation frequencies the circuit capacitances C_2 and C_3 may be partially or completely formed by parasitic capacitances of the transistor and circuit wiring. At the same time, the intrinsic Q factor of such a miniature resonator increases from 80 to 110 with a frequency increase in the range of 0.1–6.0 GHz. To exclude the penetration of high-frequency oscillations from the oscillator into the unipolar power-supply bus, a choke L_1 and a shunting capacitor C_6 are used. Variations of oscillation amplitude are registered by the full-wave rectifier envelope detector based on diodes D_1, D_2 and a smoothing capacitor C_7.

As inductive elements of the heterogeneous resonator, three designs of microstrip lines were studied, whose sections are shown in Fig. 2, designs are protected by a Russian patent [23]. The inductive elements and the oscillator are manufactured on a common FR4 printed-circuit board (PCB), whose relative permittivity is $\varepsilon = 4$. All the elements of the oscillator and detector are placed on the upper side of the board, while the lower metallized side serves as the shield with a measuring hole with a 0.8-mm diameter directly under the center of the strip conductor of the inductive element. This hole provides measurements of the FMR spectrum from a local area of ~0.5 mm^2.

The first design of of the microstrip inductor (Fig. 2a) uses a single-layer PCB made of a metallized plate with a thickness of $h = 0.5$ mm, which provides the required rigidity of the structure with its dimensions of 30 × 24 mm. However, to reduce the resonator volume, the microstrip inductor has a width of only 0.8 mm and is placed in a rectangular groove, which

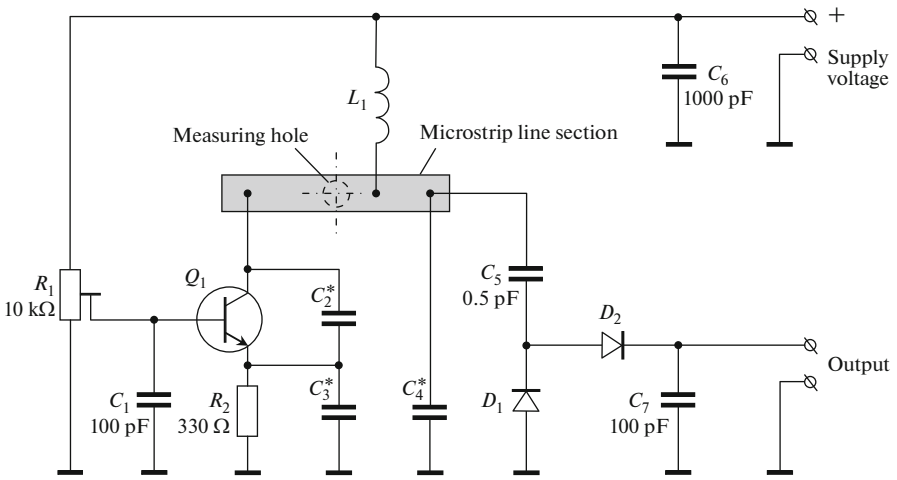

Fig 1. The circuit diagram of the measuring probe of the scanning FMR spectrometer: (Q_1) FU690F and (D_1, D_2) BAT62.

was milled to a depth of 0.3 mm. The ends of the strip conductor are connected to the contact pads on the upper side of the PCB. It is obvious that the simplicity of manufacturing a single-layer PCB is an advantage of this design of the inductive element. The disadvantages of the design include the milling modification of the board, and most importantly, the need to manufacture a conductor and install it manually by soldering so that the measuring hole is located exactly at the center of the conductor. In addition, the conductor must be placed strictly along the axis of the board, since an angular deviation leads to an unacceptable violation of the orthogonality of the orientations of the high-frequency field in the resonator and the sweeping magnetic field.

These disadvantages are eliminated in the second design of a miniature inductor created in an additional intermediate layer of a two-layer PCB (Fig. 2b). The segment of a microstrip line is manufactured using the standard technology for manufacturing multi-layer PCBs. To access the conductor, a through-milled groove is made on the upper layer of the board and, as in the above version, the ends of the inductor are soldered to the contact pads on the upper side of the PCB. This design easily ensures high accuracy of the position of the microstrip inductor relative to the measuring hole in the shield.

However, a disadvantage of the considered design is also the need for the manual operation of soldering the ends of the conductor of the inductor to the contact pads on the upper layer of the board, which have an area of at least 1 mm^2 to ensure a reliable connection. In addition, these pads form a parasitic capacitance of more than 0.1 pF with the shield, which limits the upper frequency of the oscillator to ~3 GHz, as in the first design of the inductive element. In addition, the inductance of the oscillatory circuit of the oscillator increases in proportion to the length of the conductors that connect the microstrip segment with the contact pads, thus leading to an additional decrease in the resonant frequency. We note that for this design of the inductive element, the oscillator has a frequency of 1.8 GHz with the following capacitance values indicated with asterisks in Fig. 1: $C_2 = 0.5$ pF, $C_3 = 2.0$ pF, and $C_4 = 4.7$ pF.

The third version of the inductive-element design on a two-layer PCB lacks the above disadvantages. In this design, the connections between the ends of the inductor on the intermediate layer with contact pads on the upper layer are made using blind via holes with a diameter of 0.2 mm with 0.4-mm-diameter contact pads on the upper side of the board (Fig. 2c).

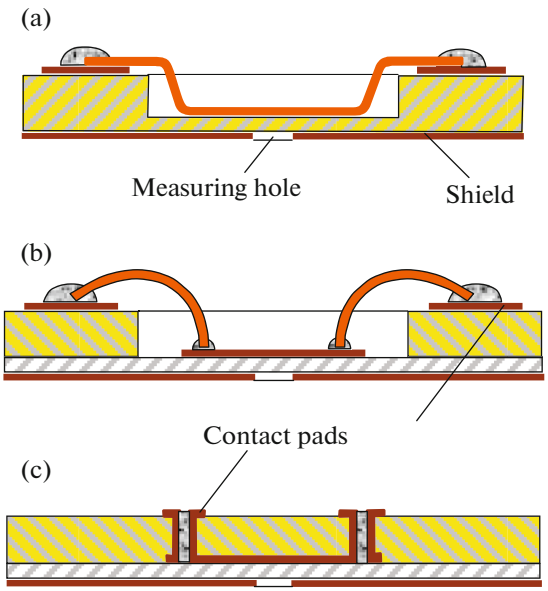

Fig. 2. The design of the inductive element of the oscillatory circuit: (a) on a single-layer circuit board and (b, c) on two-layer circuit boards.

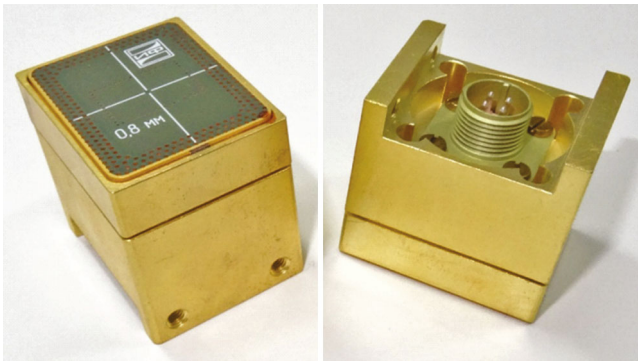

Fig. 3. Photographs of the measuring microwave probe: (left) on the side of the printed-circuit board and (right) on the opposite side.

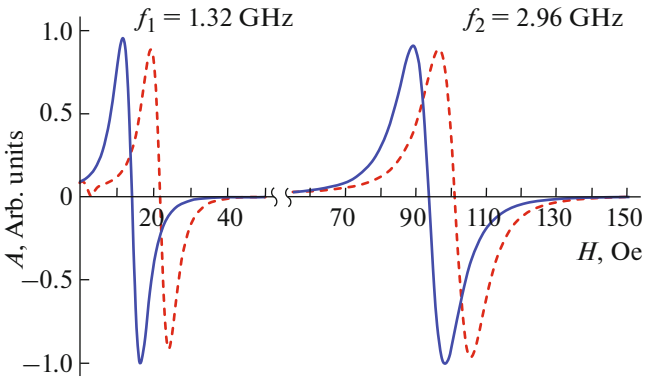

Fig. 4. Ferromagnetic resonance spectra measured at two frequencies with the magnetic-field sweep along the anisotropy axis (solid lines) and orthogonally to it (dashed line).

The use of vias makes it possible to reduce the parasitic capacitance by almost tenfold and increase the upper frequency of the probe oscillator to ~6 GHz. The main advantage of this design of the inductive element is the complete absence of manual operations during its manufacture, which is very important for mass production. It should be noted that at frequencies below 3 GHz, the design of the inductive element of the resonator almost does not affect the sensitivity of the probe; therefore, the choice of the element in this case is determined only by the technological capabilities of its manufacture.

The PCB is attached to the brass body of the probe by soldering, which provides a mechanical strength and a reliable electrical contact. For this purpose, a ~3-mm-wide strip conductor that is applied to the upper layer of the board along the entire contour is connected to the shield through an array of vias. Photos of one of the manufactured probes that are taken at two angles for clarity are shown in Fig. 3. The left image shows the measuring hole at the center of the PCB shield, while the right image shows the connector with contacts through which power is supplied to the probe and the output signal is picked off. Four threaded holes in the body allow the probe to be attached to the holder of the scanning FMR spectrometer [13, 14].

THE RESULTS OF TESTING THE PROBES

The probes were tested on a sample of an ordinary magnetic film with a thickness of 50 nm that was obtained by magnetron sputtering of a Permalloy target with a percentage–weight $Ni_{80}Fe_{20}$ composition. The film was deposited through a mask with a window area of 10 × 10 mm^2 on a square quartz glass substrate with a size of 12 × 12 mm and a thickness of 0.5 mm. The low uniaxial magnetic anisotropy in the film plane that is necessary for the operation of numerous devices based on TMFs [1, 4, 8], was induced by a planar uniform DC magnetic field of 200 Oe applied along one of the sides of the substrate during the sample deposition.

Figure 4 shows the FMR spectra that were measured on the central area of the film at two frequencies when sweeping the planar DC magnetic field H in the direction of the axis of the induced magnetic anisotropy, the easy magnetization axis (EA), and in the orthogonal direction of the hard magnetization axis (HA). In this case, the resonant fields measured at the frequency f_1 = 1.32 GHz are H_{EA} = 14.29 Oe and H_{HA} = 21.83 Oe; at the frequency f_2 = 2.96 GHz, H_{EA} = 93.76 Oe and H_{HA} = 101.02 Oe. We note that the microwave probes that were used in the experiment make it possible to record the FMR field and the width of the FMR lines ΔH with accuracies no worse than ±0.01 Oe and no worse than ±0.02 Oe, respectively.

It is known that the linewidth represents the damping parameter of the magnetization precession and is one of the most important characteristics of magnetic materials. The measured linewidths for the studied film are ΔH_1 = 4.68 Oe at the frequency f_1 and ΔH_2 = 9.26 Oe at f_2. It is also known that many magnetic characteristics of a TMF, i.e., the value of H_a and the direction θ_a of the uniaxial magnetic anisotropy, can be calculated from the measured dependence of the resonant field H_R on the angle of the direction of the DC scanning magnetic field θ_H [14]. To do this, we use the formula that relates the field H_R to the magnetic characteristics of the sample at the pump frequency f [24], excluding the unidirectional anisotropy field from it:

$$\left(\frac{2\pi f}{\gamma}\right)^2 = [H_R\cos(\theta_H - \theta_M) + H_a\cos 2(\theta_a - \theta_M)] \times [4\pi M_S + H_R\cos(\theta_H - \theta_M) + H_a\cos^2(\theta_a - \theta_M)]. \quad (2)$$

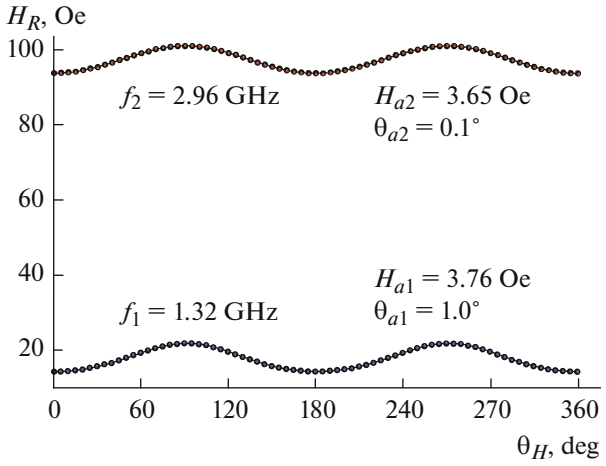

Fig. 5. The dependences of the ferromagnetic resonance field on the direction angle of the DC magnetic field of the scan measured at two frequencies.

Here, γ is the gyromagnetic ratio, M_S is the effective saturation magnetization, and the equilibrium direction θ_M of the film saturation magnetization is determined from the equation:

$$H_R \sin(\theta_H - \theta_M) + \frac{1}{2} H_a \sin 2(\theta_a - \theta_M) = 0, \qquad (3)$$

which is derived from the condition of the minimum of the film free-energy density [23].

For illustration, the dots in Fig. 5 represent the angular dependences of $H_R(\theta_H)$ that were measured at two frequencies. The measurements were performed with 5° increments on a local area at the center of the film. Solid lines show the theoretical dependences based on formulas (2) and (3) using a program in which the magnetic parameters of the films were selected automatically according to the criterion of the best match between the theory and the experiment. In Fig. 5, the values of H_{a1}, H_{a2} and the angles θ_{a1}, θ_{a2} of the uniaxial magnetic anisotropy directions for the area measured at two frequencies are indicated near the curves. It can be seen that these values for the two curves differ markedly, given that a large number of measured points increases the absolute accuracy in determining the anisotropy field and the angle of the anisotropy direction to a value no worse than ±0.01 Oe and no worse than ±0.05°, respectively.

The main advantage of the FMR scanning spectrometer is the ability to visualize the distributions of inhomogeneities in the magnetic characteristics of TMFs over the sample area by measuring the angular dependences of the resonant field $H_R(\theta_H)$ on each local area with specified increments along the axes. Figure 6 shows the distributions of the fields H_{a2} and the angles θ_{a2} of the uniaxial magnetic anisotropy direction over the area of the test sample that were measured with a step of 0.5 mm along the x and y axes.

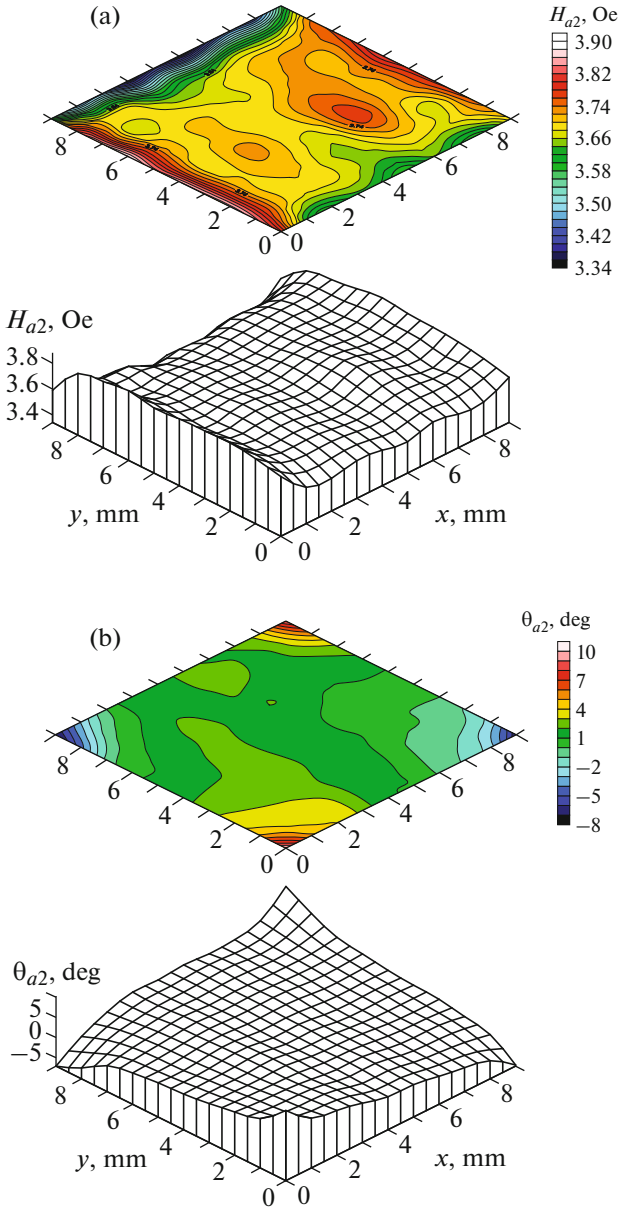

Fig. 6. The distributions of the field H_{a2} (a) and the direction angle θ_{a2} (b) of the uniaxial magnetic anisotropy over the sample area measured with an increment of 0.5 mm at the frequency f_2 = 2.96 GHz of the microwave probe.

These measurements were conducted using a microwave probe at the frequency f_2 = 2.96 GHz; however, the character of the distribution of inhomogeneities in these characteristics over the film area almost does not differ from the character of the distributions of H_{a1} and θ_{a1} that were measured with the probe at the frequency f_1 = 1.32 GHz. At the same time, a slight difference of the direction angles θ_{a1} and θ_{a2} of the uniaxial anisotropy, which does not exceed ±2°, is observed; the anisotropy field H_{a1} on all local

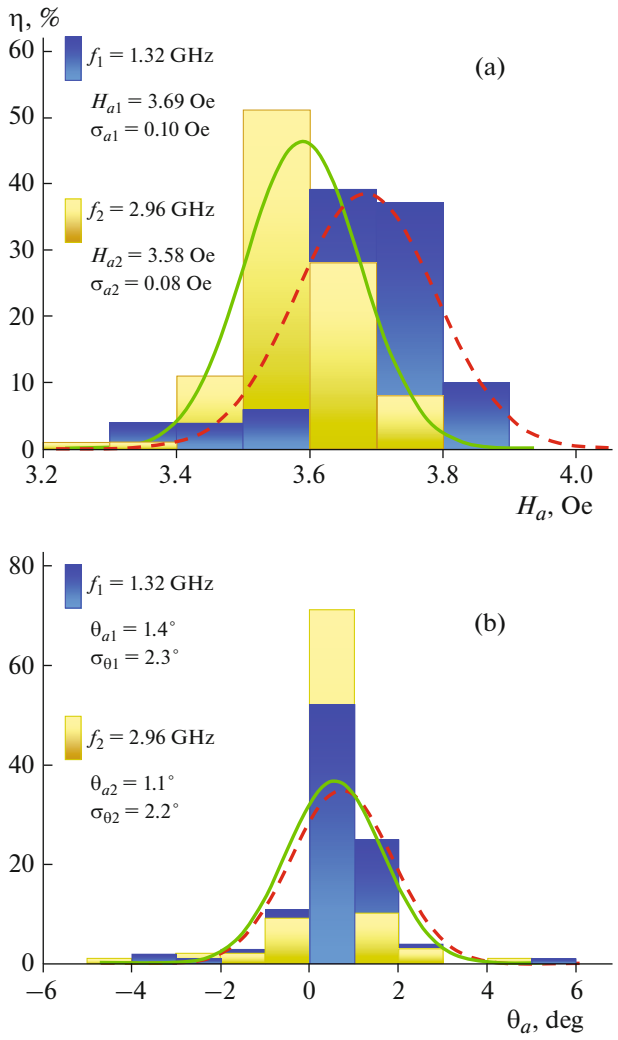

Fig. 7. The statistical distributions of the (a) fields and (b) angles of the uniaxial magnetic anisotropy over the film area at two frequencies: f_1 (dashed line) and f_2 (solid line).

areas is somewhat higher than the field H_{a2}, but this excess is at most 0.4 Oe.

It is well known that any inhomogeneities of the magnetic parameters over the TMF area are sources of noises that impair the performance of devices based on them. Therefore, the statistical characteristics of the observed inhomogeneities are important when refining the technology for producing films with uniform magnetic parameters throughout the sample. The study of the behavior of these characteristics when varying the technological conditions is also necessary for understanding the nature of the occurrence of magnetic inhomogeneities.

Figure 7 shows the diagrams that were obtained as a result of statistical processing of ensembles of the values of H_{a1}, H_{a2} and θ_{a1}, θ_{a2} that were measured over the area of the test permalloy-film sample. The diagrams $\eta(H_a)$ and $\eta(\theta_a)$ show the relative number of local areas where the measured parameters fall within the intervals of values equal to the widths of the corresponding columns. In this case, the widths of the intervals were equal to 1/10 of the range of the measured magnetic-parameter values.

As is seen, the mathematical expectations of the anisotropy field H_{a1} = 3.69 Oe and the anisotropy angle θ_{a1} = 1.4° in the ensemble of measurements at the frequency f_1 differ from the corresponding values obtained in measurements at the frequency f_2: H_{a2} = 3.58 Oe and θ_{a2} = 1.1°. In this case, the variances of the magnetic-anisotropy field σ_{a1} and angle $\sigma_{\theta1}$ that were calculated from the measurement results at the frequency f_1 exceed the corresponding values of σ_{a2} and $\sigma_{\theta2}$ for the frequency f_2.

The results show that the angular and amplitude variances of the uniaxial magnetic anisotropy that are caused by the imperfect technologies for obtaining TMFs, due to their small values, almost cannot be detected by measuring the magnetic parameters of local areas of samples using the FMR method at frequencies of the centimeter wavelength range, as was proposed in [1, 11, 12]. In this range, not only are the resonant fields too high and reach values of ~10^3 Oe, but the FMR linewidth also increases to 10^2 Oe, thus not allowing measurements of the TMF characteristics with a required accuracy.

A significant increase in the accuracy of measuring the resonant fields of local TMF areas by the scanning FMR spectrometer using the developed probes [23] in comparison to the known–probes [13, 14] is shown in Fig. 8. The dependences of the FMR fields on the direction angle of the DC scanning magnetic field that were measured on a 16-nm-thick cobalt film, which was obtained by chemical deposition are also given here [24]. The round dots show the measurement results on the probe–analog at a frequency of 2.274 GHz and a diameter of the measuring hole of 1 mm [24]; triangular dots correspond to an analog at a frequency of 2.295 GHz (for an objective comparison of the results) with a diameter of the measuring hole of 0.8 mm. The experimental points were used to perform theoretical approximations of these dependences using formulas (2) and (3) and obtain the values of H_a and the angle of direction θ_a of the uniaxial magnetic anisotropy (see Fig. 8), which have noticeably different values. Despite the fact that the probe–analog picks signals off an area that is 1.6 times larger than the developed probe, its noise is one order of magnitude higher and reaches ±2 Oe.

CONCLUSIONS

The developed designs of the measuring probes for the scanning FMR spectrometer have a sensitivity that exceeds that of the prototype by approximately one order of magnitude [13]. This made it possible to improve the quality of visualization of the distribu-

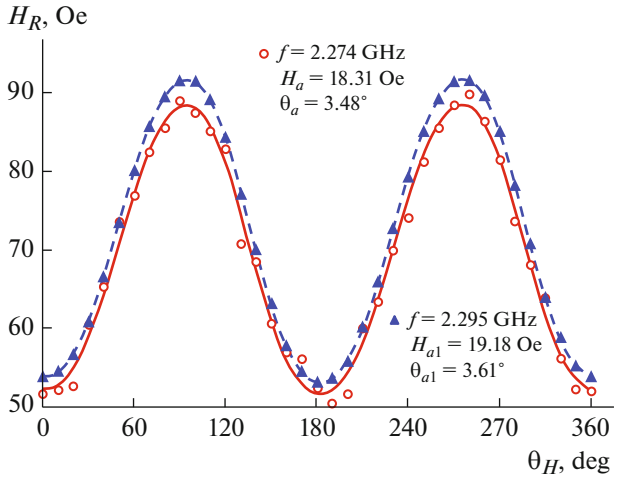

Fig. 8. The dependences of the FMR fields of the cobalt film on the direction angle of the DC magnetic field of the scan measured using a probe–analog (round dots) and the studied probe (triangular points). Lines are approximations by formulas (2) and (3).

tions of inhomogeneities of the magnetic characteristics over the sample area due to a significant increase in the measurement accuracy on local areas. The degree of measurement locality is determined by the diameter of the hole in the shield of the miniature resonator in the range of 0.1–1.0 mm, which simultaneously serves as the source of a high-frequency magnetic field and a communication channel between the measured film area and the resonator. The signal-to-noise ratio for a probe with a hole diameter of 0.8 mm, which was measured on a permalloy film with a thickness of 5 nm, is at least 10 dB.

The existing ability of a set of replaceable probes to cover a wide frequency range of 0.1–6.0 GHz is especially important in the study of metal magnetic films. It is known that when studying such films on mass-produced spectrometers that operate in the centimeter wavelength range at frequencies of the order of 10^{10} Hz, difficulties arise due to the small thickness of the skin layer, which additionally decreases further near the FMR due to an increase in the magnetic permeability of the sample. As a result, the shape of the resonance curve can be strongly distorted. However, the use of the developed probes allows one to significantly decrease the pump frequency without reducing the sensitivity of the spectrometer; in this case, the skin depth accordingly increases, and this problem disappears.

The efficiency of using the developed probes to study the nature and features of the distribution of magnetic inhomogeneities over the sample area was demonstrated by measuring the parameters of the uniaxial magnetic anisotropy on a permalloy film 50 nm thick and 10 × 10 mm in size. The film was scanned over the entire area in 0.5-mm increments by two probes with different frequencies and with the same measuring holes with a 0.8-mm diameter. The high accuracy of measurements of the magnitude and direction of the uniaxial magnetic anisotropy was demonstrated. The results presented in this paper will undoubtedly be useful in solving a number of technological, engineering, and many scientific problems that are related to the creation of new magnetic materials with specified properties and the development of devices based on them.

FUNDING

This study was supported by the Ministry of Science and Higher Education of the Russian Federation as part of a complex project on the development of high-technology production facilities (agreement no. 075-11-2019-054, November 22, 2019).

REFERENCES

1. Soohoo, R.F., *Magnetic Thin Films,* New York: Harper and Row, 1965.
2. Karpenkov, S.Kh., *Tonkoplenochnye magnitnye preobrazovateli* (Thin-Film Magnetic Transducers), Moscow: Radio i Svyaz', 1985.
3. Babitskii, A.N., Blinnikov, E.P., Vladimirov, A.G., Gitarts, Ya.I., Polyakov, V.V., and Frolov, G.I., *Geofiz. Appar.,* 1991, no. 94, p. 21.
4. Babitskii, A.N., Belyaev, B.A., Boev, N.M., Skomorokhov, G.V., Izotov, A.V., and Galeev, R.G., *Instrum. Exp. Tech.,* 2016, vol. 59, no. 3, pp. 425–432. https://doi.org/10.1134/S0020441216030131
5. Zubkov, V.I. and Shcheglov, V.I., *J. Commun. Technol. Electron.,* 2011, vol. 56, no. 7, p. 853. https://doi.org/10.1134/S1064226911070151
6. Ustinov, A.B., Nikitin, A.A., and Kalinikos, B.A., *Tech. Phys.,* 2015, vol. 60, no. 9, p. 1397. https://doi.org/10.1134/S1063784215090224
7. Fetisov, Yu.K. and Sigov, A.S., *RENSIT Radioelektron., Nanosist., Inf. Tehnol.,* 2018, vol. 10, no. 3, p. 343. https://doi.org/10.17725/rensit.2018.10.343
8. Belyaev, B.A., Izotov, A.V., Leksikov, An.A., Solov'ev, P.N., and Tyurnev, V.V., *Izv. Vyssh. Uchebn. Zaved., Fiz.,* 2020, vol. 63, no. 9, p. 7.
9. Hamida, A.B., Sievers, S., Pierz, K., and Schumacher, H.W., *J. Appl. Phys.,* 2013, vol. 114, p. 123704-1. https://doi.org/10.1063/1.4823740
10. Tamaru, S., Tsunegi, S., Kubota, H., and Yuasa, S., *Rev. Sci. Instrum.,* 2018, vol. 89, p. 053901-1. https://doi.org/10.1063/1.5022762
11. Frait, Z., *Czech. J. Phys.*, 1959, vol. 9, p. 403.
12. Soohoo, R.F., *J. Appl. Phys.,* 1962, vol. 33, p. 1276.
13. Belyaev, B.A., Leksikov, A.A., Makievskii, I.Ya., and Tyurnev, V.V., *Instrum. Exp. Tech.,* 1997, vol. 40, no. 3, pp. 390–394.
14. Belyaev, B.A., Izotov, A.V., and Leksikov, A.A., *IEEE Sens. J.,* 2005, vol. 5, no. 2, p. 260. https://doi.org/10.1109/JSEN.2004.842293
15. Belyaev, B.A., Izotov, A.V., and Kiparisov, S.Ya., *JETP Lett.,* 2001, vol. 74, no. 4, pp. 226–230.

16. Belyaev, B.A. and Izotov, A.V., *JETP Lett.,* 2002, vol. 76, no. 3, pp. 174–179.

17. Belyaev, B.A., Izotov, A.V., Skomorokhov, G.V., and Solovev, P.N., *Mater. Res. Express,* 2019, vol. 6, p. 116105-1. https://doi.org/10.1088/2053-1591/ab4456

18. Belyaev, B.A., Boev, N.M., Izotov, A.V., Skomorokhov, G.V., and Solov'ev, P.N., *Izv. Vyssh. Uchebn. Zaved., Fiz.,* 2020, vol. 63, no. 1, p. 17. https://doi.org/10.17223/00213411/63/1/17

19. Belyaev, B.A., Tyurnev, V.V., Izotov, A.V., and Leksikov, An.A., *Phys. Solid State,* 2016, vol. 58, no. 1, pp. 55–61. https://doi.org/10.1134/S1063783416010054

20. Belyaev, B.A. and Izotov, A.V., *JETP Lett.,* 2016, vol. 103, no. 1, pp. 41–45. https://doi.org/10.1134/S0021364016010033

21. Belyaev, B.A., Izotov, A.V., Solovev, P.N., and Boev, N.M., *Phys. Status Solidi RRL,* 2020, vol. 14, p. 1900467-1. https://doi.org/10.1002/pssr.201900467

22. Abragam, A. and Bleaney, B., *Electron Paramagnetic Resonance of Transition Ions,* Oxford: *Clarendon Press*, 1970.

23. Belyaev, B.A., Boev, N.M., and Izotov, A.V., RF Patent 2691996, *Byull. Izobret.,* 2019, no. 17.

24. Belyaev, B.A., Izotov, A.V., Kiparisov, S.Ya., and Skomorokhov, G.V., *Phys. Solid State,* 2008, vol. 50, no. 4, pp. 676–683.

Translated by A. Seferov